Stability Effects of Frequency Controllers and Transmission Line Configurations on Power Systems with Integration of Wind Power

by

Hussein Mohamed Abdelhalim

B.S. Electrical Engineering
University of Florida, 2010

Submitted to the Department of Electrical Engineering and Computer Science
in partial fulfillment of the requirements for the degree of

Master of Science in Electrical Engineering and Computer Science

at the

MASSACHUSETTS INSTITUTE OF TECHNOLOGY

September 2012

Author .....
Hussein Mohamed Abdelhalim
Department of Electrical Engineering and Computer Science

Certified by .....
Kamal Youcef-Toumi
Professor of Mechanical Engineering
Thesis Supervisor

Certified by .....
Amro Farid
Assistant Professor of Engineering Systems & Management, Masdar Institute
Thesis Co-Supervisor

Accepted by .....
Leslie A. Kolodziejski
Chair, Department Committee on Graduate Students

Stability Effects of Frequency Controllers and Transmission Line Configurations on Power Systems with Integration of Wind Power

Hussein Mohamed Abdelhalim

Submitted to the Department of Electrical Engineering and Computer Science
on August 31st, 2012, in partial fulfillment of the requirements for the degree of
Master of Science in Electrical Engineering and Computer Science

Abstract

This thesis investigates the stability effects of the integration of wind power on multi-machine power systems. First, the small-signal stability effects of turbine governors connected to synchronous generators in the presence of large-scale penetration of wind and load power disturbances are analyzed. Results suggest that tuning the turbine governors when wind power generation is present can improve the small-signal stability of an interconnected system. Then, the transient stability effects of integrating doubly-fed induction wind turbine generators through different transmission line configurations and at different buses are analyzed. Results show that connecting the wind through transmission lines and to different buses introduces a delay in the oscillatory response of the synchronous generator speed, and bus voltage oscillations are also affected. Results also show that there is no significant effect on the base cases when using different interconnection voltages to connect the wind. Overall, the results can be used by power system operators when making decisions on turbine governor tuning and transmission line configurations when connecting wind farms to existing power systems while optimizing for small-signal and transient stability response.

Thesis Supervisor: Kamal Youcef-Toumi
Title: Professor of Mechanical Engineering

Acknowledgements

I would like to thank my adviser, Professor Kamal Youcef-Toumi, for his support. Professor Kamal always inspired me to think outside the box when looking at problems. His feedback, insights, and attention to detail has truly made me a better researcher.

I would also like to thank Professor Amro Farid for being a second adviser and excellent mentor. Thank you for sharing the details of this project and bringing me on board when I was looking for a research group in the area of renewable energy and power systems. I am grateful for the weekly (and sometimes a lot more often) meetings, research direction, constant support, and feedback of my work.

I would also like to thank Dr. Ambrose Adegbege for his mentorship and guidance. I appreciate the constant feedback of my work and for the long technical discussions that helped me focus in on my research objectives. I am also grateful to Professor Luis Rouco for his strong collaboration. I appreciate you meeting with me regularly during your time here at MIT and continuing to be a valuable resource after returning to Spain.

I would like to thank my colleagues in the research groups at both MIT and Masdar. I enjoyed our daily conversations and in sharing tips and tricks that made us all more efficient. I would also like to thank all of my friends, both at MIT and elsewhere, for making my graduate school experience more enjoyable.

This thesis would not have been possible if it were not for the love and encouragement of my entire family. They were always there for me in both easy and difficult times. I would like to dedicate this work to my father, who passed away a few months before it was completed. He inspired me to pursue electrical engineering and to strive for the top in personal, academic, and professional settings. I am forever grateful for his support as a friend and mentor throughout my life.

My acknowledgements would not be complete without thanking God for the constant support and blessings.

Table of Contents

List of Figures

List of Tables

Chapter 1

Introduction

1.1 Research Motivation

The use of wind energy in the last couple of decades has increased substantially. In the 1990s, worldwide wind capacity doubled approximately every three years, and capacity has continued to grow by approximately 25% each year in the past decade [1].Over the same period, costs have been decreasing by an average of 30% per year. The level of sophistication associated with wind turbine technology has also evolved significantly over the past decade. Larger, more reliable wind turbines continue to enter the market at a fraction of the cost of turbines from the 1980s and 1990s. In order to maximize the use of the rapid development and growth of the wind turbine technologies, researchers are needed to study the impact that high penetration of wind energy has on existing power networks.

Many technical issues arise when integrating wind power into an electric grid. Technical issues can occur at different time scales. Small-signal and transient stability concerns associated with small and large disturbances occur on the millisecond and second timescale. The intermittency of the wind speed and it's impact on the interconnected power network occurs on the order of minutes or hours. Another technical issue that arises with wind are the dynamics introduced by the doubly-fed induction generator onto the synchronous generators already present in the system.

1.2 Research Objectives and Questions

There are two main research objectives in this thesis:

1. Analyze the small-signal stability effects of turbine governors on power systems with integration of wind power
2. Analyze the transient stability effects of modified transmission line configurations on power systems with integration of wind power

A series of high-level research questions must be addressed in order to be able to achieve the research objectives. The first two questions listed below cover both research objectives, while the next two questions individually address each of the objectives respectively.

- What device models can be used to study power system stability effects? What assumptions are taken in these models?
- What are the similarities/differences of small-signal stability and transient stability?
- What impact will the introduction of wind have on the equations associated with turbine governor control on synchronous generators? How will any change impact the power system following a small-signal disturbance?
- What impact will the modified transmission line configurations have on the power flow and device model equations? How will any change impact the power system following a large disturbance?

1.3 Research Approach and Organization of Thesis

The research approach taken here was to learn the mathematical background associated with the different device models and analysis techniques in parallel with running simulations on already existing power system models. Linking the theory with the application early on in the research process was essential in uncovering many of the subtleties and nuances associated with the integration of the different device models into the system state model. The research approach also helped in gaining proficiency using the

various power system software tools quicker and in better understanding the simulations presented in the literature. Finally, this synchronized approach of combining theory with application from the beginning made it easier to identify research objectives more quickly as it became apparent relatively early on where there was a gap in the literature that could be addressed by running certain simulations.

There are three additional chapters in the thesis. Chapter 2 addresses the first research objective listed in Section 1.2 above, while Chapter 3 addresses the second research objective. The chapters are organized in such a way that each is fully encompassing and can be read separately. All of the device models used are summarized, and additional details not included are carefully referenced. The various analysis techniques and test systems used are introduced and defined physically and analytically.

Since small-signal stability analysis and transient stability analysis are distinct issues, organizing the chapters in this way is beneficial as future researchers can focus exclusively on their topic of interest. The organization of the chapters using this approach also allows the reader to compare and contrast similarities and differences of the two analysis techniques easily. Finally, Chapter 4 includes a conclusion and a section on potential future work that can build off this thesis.

1.4 Novelty of Research Contributions

There are novel research contributions addressing both of the objectives listed in the first section. With respect to the first objective dealing with the small-signal stability effects of turbine governors, the main research contribution was modifying the droop equation to take into account rated power contributions from the wind induction generator units. Traditionally, the droop equation had only considered rated power contributions from conventional synchronous generator machines. Many of the results obtained from the simulations were also novel, as the inclusion of deep penetration of wind power and it's relation to the turbine governors had not previously been investigated in great detail.

With respect to the second objective dealing with the transient stability effects of modified transmission line configurations, the main research contribution was analyzing alternative, more likely scenarios of how the wind might actually be connected to an existing power system. Previous research had analyzed the base case where doubly-fed induction generators are directly connected to synchronous generator buses, and this assumption was challenged in the thesis. Results obtained from looking at the different scenarios can be used by power system to determine the best placement of wind farms when optimizing for enhanced transient stability. All of these contributions will become more apparent and explained in more detail in the following two chapters.

Chapter 2

Small-Signal Stability Effects of Turbine Governors on Power Systems with Integration of Wind Power

The turbine governor is the primary frequency controller of a synchronous machine. The stability effects of turbine governors on traditional power systems are well known. However, the integration of wind farms into the grid has introduced new dynamics into the power system that must be taken into account when tuning these controllers. This chapter summarizes existing power system models and analyzes the small-signal stability effects of the turbine governors connected to the synchronous generators in the presence of large-scale penetration of wind and load power disturbances. A case study is presented where the effects of the turbine governor are evaluated in the presence of a 20% increase in load active and reactive power for the IEEE 14-bus system. Results suggest that tuning the turbine governors when wind power generation is present can improve the small-signal stability of an interconnected system.

2.1 Introduction

A power system's dynamic behavior is determined mainly by the generators. Conventional, thermal power plants are typically represented by synchronous generators, while modern wind turbines are typically represented by induction generators. Synchronous generators have various distributed, local frequency and voltage controllers connected to the

machines at the power system bus level. Overall, the purpose of the controllers is to maintain synchronism and system stability when the system is subject to a disturbance [2]. The large-scale integration of wind power into the electric grid will change the dynamics of a power system since the interaction of induction generators with the system is different than that of synchronous generators [1]. This may alter the effects of the synchronous generator controllers, potentially causing the need to adjust or tune them in order to maintain synchronism and system stability when the system is subject to a disturbance.

The focus of this chapter is on frequency control. The primary frequency controller of the synchronous generator is the turbine governor (TG) [3]. The effects of the turbine governor controllers on conventional power systems containing only synchronous generators are well known, and a summary of these effects is presented in the following section. After understanding these effects, we extend the equations to include the introduction of power generated from doubly-fed wind turbine induction generators (DFIGs) in order to analyze the small-signal stability of an interconnected power system in the presence of a load disturbance.

Details of the models considered for the different generators and a model for the turbine governor are provided in Section 2.2. Techniques for tuning the controllers in the presence of both synchronous and induction generators are also presented in Section 2.2. In Section 2.3, the previously summarized device models are integrated into a system model, and analysis techniques in the presence of different types of disturbances are discussed. Finally, a case study using the IEEE 14-bus system is presented in Section 2.5, and a conclusion is provided in Section 2.6.

2.2 Machine and Controller Modeling

This section summarizes the machine models for the synchronous generator used to represent a thermal generating unit and a doubly-fed induction generator (DFIG) used to represent a wind turbine. This section also summarizes the turbine governor, the

automatic voltage regulator (AVR) that is used for synchronous generator voltage control, and the controls associated with the DFIG wind turbine.

2.2.1 Synchronous Machine Model

Synchronous machine models of varying sophistication and detail have been reported in the literature. The most basic model is the classical model, which can be represented as a second order system with the following differential equations

$$\dot{\delta} = \Omega_b(\omega - 1) \tag{1}$$

$$\dot{\omega} = \frac{(p_m - p_e - D(\omega - 1))}{M} \tag{2}$$

where

δ : rotor angle

ω : rotor speed

Ω_b : base frequency

p_m, p_e : mechanical power, electrical power

D : damping coefficient

M : mechanical starting time ($M = 2H$)

H : inertia constant

Model comparisons, detailed modeling, and the explanation of assumptions for higher-order versus reduced-order models can be found in various references [4–6]. The drawback of the classical 2nd order model is that it neglects all electromagnetic dynamics. For our purposes, we have chosen to use a 6th order model to represent the synchronous machines because the model includes transient and subtransient phenomena that should be accounted for in stability analysis. The 6th order model is described by (1) and (2) along with differential equations for transient voltages $\dot{e}_q'$ and $\dot{e}_d'$ and subtransient voltages $\dot{e}_q''$ and $\dot{e}_d''$. These variables represent the dynamics of the dc field winding and of the rotor core induced currents and the fast dynamics of damper windings respectively. Full derivation and details on this model can be found in [6-7].

In addition to the six differential equations, the machine model also has six algebraic equations for the following variables: active power p, reactive power q, bus voltage magnitude v, bus voltage angle θ, mechanical power p_m and field voltage v_f. In order to interface with controller device models, auxiliary equations for the field voltage v_f and the mechanical torque τ_m are defined below where τ_{m0} and v_{f0} are the synchronous machine initialized values.

$$0 = \tau_{m0} - \tau_m \tag{3}$$

$$0 = v_{f0} - v_f \tag{4}$$

The initialization chain of the synchronous machine and corresponding controllers are provided in Figure 2.1 below [4].

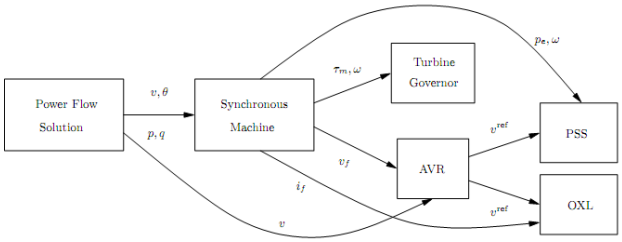

Figure 2.1: Initialization Chain of Synchronous Machines

The synchronous machine algebraic equations are initialized using results from the power flow analysis, while the TG and AVR controllers are initialized using synchronous machine variables. Secondary voltage controllers, such as the power system stabilizer (PSS) and over excitation limiters (OXL) are initialized using AVR reference variables.

For the purposes of studying the effects of frequency control, a synchronous generator can be represented as a large rotating mass with two opposing torques, acting on the rotation [3]. The electrical torque, τ_e , acts to slow down the rotational speed, ω, while the mechanical torque τ_m, acts to speed it up. When τ_e and τ_m are equal in magnitude, ω is constant. However, a disturbance on the system can cause the electrical load to increase. The system will no longer be in equilibrium as τ_e will become greater than τ_m, and the entire rotating system will start slowing down. In order to restore equilibrium, frequency controllers are needed.

2.2.2 Synchronous Generator Controller Models

The main purpose of this section is to discuss primary frequency control using the turbine governor. Voltage control using the automatic voltage regulator (AVR) is also briefly discussed. Although voltage control is not the primary focus of this chapter, understanding the basics of the AVR is essential since it is incorporated in the system model.

2.2.2.1 Turbine Governor

As discussed in the previous section, load changes can cause the system frequency to drift outside acceptable limits. The purpose of the frequency governing mechanism is to sense the machine speed and adjust the input valve in order to change the mechanical power output. Ideally, this adjustment will compensate for the load changes and restore the frequency back to it's nominal value. Mechanical power and mechanical torque are related by the equation below.

Primary frequency control is implemented on a purely local level. This means that there is no coordination between different generating units in systems with multiple synchronous generators. Figure 2.2 below shows a simplified model of a synchronous machine's primary frequency control [4].

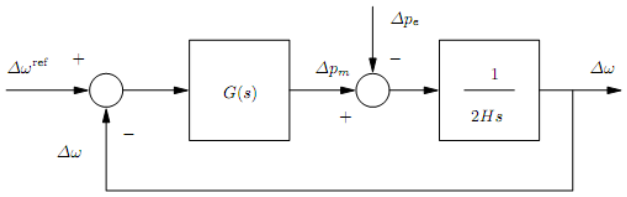

Figure 2.2: Primary Frequency Control Block Diagram

The turbine governor is the primary frequency controller for a synchronous machine. In the figure above, the transfer function G(s) depends on the type of turbine and on the control. In steady state conditions,

$$\lim_{s->0} G(s) = \frac{1}{R} \tag{5}$$

where R is the effect of the droop on the regulation. R determines the per unit change in rated power output, ΔP, for a given change in frequency as shown in the equation below.

$$R = \frac{\Delta\omega}{\Delta P} \tag{6}$$

It is important to note that ΔP is set to 1 pu in steady-state, giving a direct proportion between the droop and the change in frequency. Unit regulation is often discussed in percentages, and an example using the above equation would indicate that 3% regulation for a unit would create a 3% change in the frequency for a machine running at rated power. In the event of a load disturbance, ΔP will increase. This increase will result in the need to tune the value for R if system constraints require the change in frequency to stay within a certain range. In general, R is typically set on each generating unit so that a change in rated output will result in the same frequency change for each unit [3]. Typical machine values for R range from 0.02-0.05 [4],[8]. Figure 2.3 below shows the effect of R on the control loop. The linear relationship presented in Equation (6) when $R \neq 0$ is confirmed.

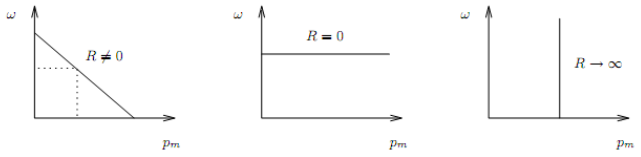

Figure 2.3: Effect of Droop *R* on the Control Loop

Almost all interconnected power systems have multiple generating units, so it is important to understand the effect when there are multiple turbine governors in a given system. The equation below shows the frequency change in the event that multiple generators with their own turbine governors are connected to the same system [3]. This equation assumes that all generating units have a turbine governor with a particular droop value.

$$\Delta\omega = \frac{\Delta P}{\frac{1}{R_1} + \frac{1}{R_2} + \ldots + \frac{1}{R_n}} \tag{7}$$

Based on the equation, we can see that the change in frequency is mitigated as the number of turbine governors is increased. This means that a system with multiple turbine governors can better regulate a sudden increase in load than a system with less turbine governors. A simplified turbine governor model is shown in the control diagram below.

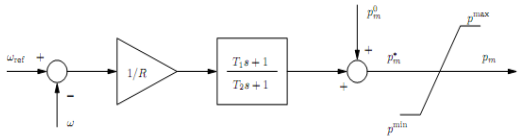

Figure 2.4: Turbine Governor Model

The variables in the diagram are defined below.

ω_{ref} : reference speed

R : droop gain

T_1, T_2 : transient and governor gain time constants

$p_m^{\ 0}, p_m$: initial mechanical power, mechanical power

$p^{\max}, p^{\min}$: maximum and minimum output power

The turbine governor can be modeled as a first order system with the following differential equation and algebraic equation [10].

$$\dot{x}_g = \frac{\frac{1}{R}(1-\frac{T_1}{T_2})(\omega_{ref}-\omega)-x_g}{T_2} \tag{8}$$

$$\hat{\tau}_m = x_g + \frac{1}{R}\frac{T_1}{T_2}(\omega_{ref}-\omega)+\tau_{m0} \tag{9}$$

The link between the TG model and the synchronous machine model is the initialized variable τ_{mo} that can be substituted into equation (3) above.

In this section, the models and tuning methodologies of the synchronous generator controllers are presented. The controllers of interest are the automatic voltage regulator, the power system stabilizer, and the turbine governor. Figure 2.5 below represents the synchronous generator and it's associated controllers using a block diagram model [4].

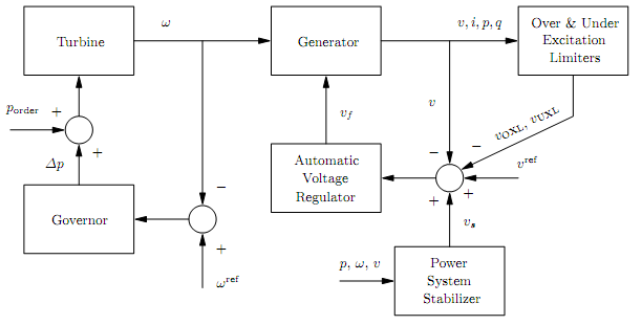

Figure 2.5: Synchronous generators and associated controllers

2.2.2.2 Automatic Voltage Regulator (AVR)

The automatic voltage regulator is the synchronous machine's primary voltage regulator. There are several different AVR models in the literature [4]. Here, we summarize a simple AVR model that can be used for stability analysis. Figure 2.6 below shows a simplified conceptual model of a synchronous machine's primary voltage control. Essentially, primary voltage regulation can be broken down into a transfer function composed of the machine's d-axis emf, the exciter, and the AVR regulator. The system's stability is determined by the AVR gain.

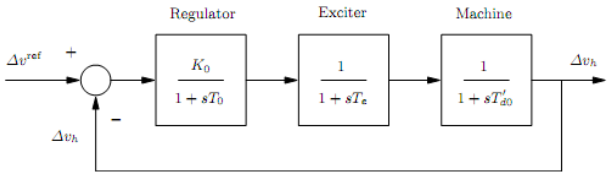

Figure 2.6: Simple model of a machine's primary voltage control

Every AVR model has the following two algebraic equations

$$0 = v_0^{ref} - v^{ref} \tag{10}$$

$$0 = \tilde{v}_f - v_f \tag{11}$$

where (11) defines the AVR reference voltage Here, we define the reference voltage explicitly as a variable because it used by secondary voltage control devices such as the power system stabilizer. (12) represents the link between the synchronous machine and the AVR. This equation substitutes into (4) as discussed above.

AVR models typically model the bus voltage measure delay as a lag block described the by the differential equation below

$$\dot{v}_m = \frac{v_h - v_m}{T_r} \tag{12}$$

where v_m is the state variable used as a voltage signal within the AVR, v_h is the generator bus voltage, and T_r is the measurement block constant. A simple AVR model is shown in Figure 2.7 below.

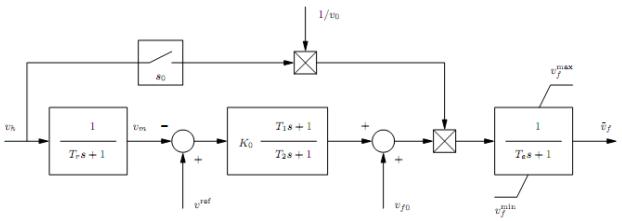

Figure 2.7: AVR Model

The model above can be described by the following set of differential equations where T_1 and T_2 represent the regulator zero and pole respectively, K_0 is the regulator gain, and T_e and T_r are the field circuit and measurement time constants respectively. More details on these equations can be found in [4].

2.2.3 DFIG Wind Turbine Model and Associated Controls

The general structure of a DFIG wind turbine model and it's associated controls is shown in Figure 2.8 below [9].

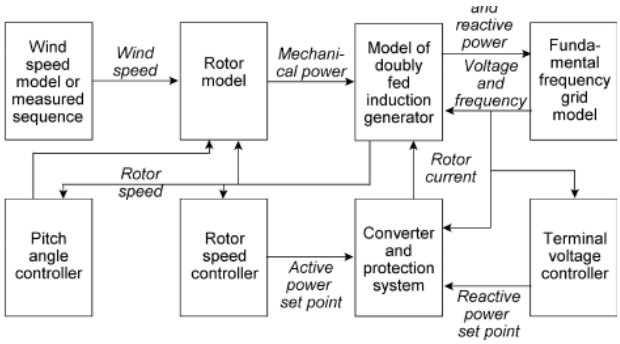

Figure 2.8: General DFIG Wind Turbine Model with Associated Controls

The wind speed can be modeled in many different ways. Here, we assume a Weibull distribution to take into account the constant variation around a nominal wind speed v_{wn} [4]. This is described by the probability density function below

$$f(v_{wn}, c_w, k_w) = \frac{k_w}{c_w^k} v_{wn}^{k-1} e^{-\left(\frac{v_{wn}}{c_w}\right)^{k_w}} \tag{13}$$

where c_w and k_w are constants defined in the wind model data matrix. Time variations of the wind speed $\xi_w(t)$ are then obtained as follows

$$\xi_w(t) = \left(-\frac{\ln \iota(t)}{c_w} \right)^{\frac{1}{k_w}} \; ; \; \iota \in [0,1] \tag{14}$$

where $\iota(t)$ is a generator of random numbers. The wind speed is then calculated using the following equation

$$v_w(t) = (1 + \xi_w(t) - \xi_w^a) v_w^a \tag{15}$$

where ξ_w^a is the average value of $\xi_w(t)$.

The wind speed is an input to the rotor model. The rotor model assumes an algebraic relationship between the wind speed and the pw, mechanical power extracted from the wind as described below where c_p is a performance coefficient function and A_r is the area swept by the rotor [9].

$$p_w = \frac{\rho}{2} c_p(\lambda, \theta) A_r v_w^3 \tag{16}$$

Mechanical power is then related to mechanical torque using the following equation where ω_m is the rotational speed.

$$\tau_m = \frac{p_w}{\omega_m} \tag{17}$$

The equation of motion for the rotor modeled as a single shaft is described by the first-order differential equation shown below.

$$\dot{\omega}_m = \frac{\tau_m - \tau_e}{2H_m} \tag{18}$$

Since converter dynamics are fast with respect to electromechanical transients, their models can be highly simplified. The converter is modeled as an ideal current source where the d and q-axis rotor currents, i_{qr} and i_{dr}, are state variables used for voltage and rotor speed control respectively. A pitch angle controller uses the actual value of the rotor speed to control the blade pitch angle. Since we are mainly interested in the effects of synchronous generator controllers in this study, the reader is referred to [9] for detailed equations on the controls associated with the DFIG wind turbine.

2.2.4 Turbine Governor Control in the Presence of Synchronous Generators and DFIGs

Unlike synchronous generators, doubly-fed induction generators do not have turbine governors. However, since the induction generators are generating units, they will also play a role in accounting for a system load disturbance. Because of this, additional work needs to be done in solving for the change in power for a system with both induction and synchronous generators before plugging in values for equation (7). The DFIG's power output should be taken into account in the event of a load disturbance since some of the additional load will be absorbed by the power generated from it. We can take the total rated power of the system, P_{TOT0}, to be the sum of the total rated power of each machine with turbine governors, P_{Y0}, and the total rated power of machines without turbine governors, P_{N0}.

$$P_{TOT0} = P_{Y0} + P_{N0} \tag{19}$$

In steady state, P_{TOT0} will equal the load power P_{L0}, assuming generation and demand are matched. In the event of a disturbance, P_{L0} will increase by some amount, ΔP_L. This is described by the equation below where P_L is the load power with the disturbance.

$$P_L = P_{L0} + \Delta P_L \tag{20}$$

If we assume that the machines share the added load proportionally, then the added amount of power required from each of the types of machines can be described by the two equations below.

$$\Delta P_Y = \frac{P_{Y0}}{P_{TOT0}} \cdot \Delta P_L \tag{21}$$

$$\Delta P_N = \frac{P_{N0}}{P_{TOT0}} \cdot \Delta P_L \tag{22}$$

Equation (7) can then be updated where $\Delta P = P_{TOT0} + \Delta P_Y$ as shown below.

$$\Delta\omega = \frac{P_{TOT0} + \Delta P_Y}{\frac{1}{R_1} + \frac{1}{R_2} + \ldots + \frac{1}{R_n}} \tag{23}$$

It is best to use per-unit quantities when solving for the equation above. We can see from the equations that the substitution of induction generator units to synchronous generator units in the system will increase P_N and decrease P_Y. Assuming the droop values of each of the synchronous generators stay constant, this will have a positive effect as the change in

frequency will decrease due to the decrease in the change of load power acting on the synchronous generators with turbine governors.

A simple example of this can be demonstrated using the following parameters:
Case 1: P_{Y0} = 900 MW, P_{N0} = 100 MW, and ΔP_L=200 MW; Case 2: P_{Y0} = 500 MW, P_{N0} = 500 MW, and ΔP_L=200 MW.
In both cases, we assume two synchronous generators with droop values of 0.05 and two induction generators. If we assume that generation matches demand in steady state, then the additional load, ΔP_L, is 20 % of total load P_L in both cases. In both cases, P_{TOT0} is equal to 1000 MW. Using this, let's first change all parameters to per-unit quantities. This yields the following:
Case 1: P_{Y0} = 0.9 pu, P_{N0} = 0.1 pu, and ΔP_L=0.2 pu;
Case 2: P_{Y0} = 0.5 pu, P_{N0} = 0.5 pu, and ΔP_L=0.2 pu.

For case 1, ΔP_Y = 0.18 and ΔP_N = 0.2. This means that the change in synchronous generator frequency will be 0.0295 or approximately 3%. For case 2, ΔP_Y = 0.1 and ΔP_N = 0.1, and the change in synchronous generator frequency will be 0.0275 or approximately 2.8%.

Alternatively, system constraints could require the operation within a certain frequency range. This often occurs in small signal stability studies where the system is assumed stable around a particular operating point, but deviations too far away from the operating point could lead to instability. In this case, a maximum value for $\Delta\omega$ would be imposed on the system, and the turbine governors could then be tuned to achieve the desired control.

A simple example of this can be demonstrated using the same parameters as discussed above with the addition of a maximum $\Delta\omega$ of 0.2 pu. Assuming that we have two synchronous generators with identically tuned turbine governors would require R_1 and R_2 to equal 0.0363 for case 1 and 0.0339 for case 2. Further analysis is presented in Section IV using a case study based on the IEEE 14-bus system.

2.3 System Model and Analysis Techniques

The non-linear differential and algebraic equations that represent the individual device models for the machines and controllers can be combined to create a system model. The general equations are shown below [10].

$$\begin{bmatrix} \dot{x} \\ 0 \end{bmatrix} = \begin{bmatrix} f(x,y,u) \\ g(x,y,u) \end{bmatrix} \tag{24}$$

where x is the vector of state variables that typically include the machine model dynamics and controller dynamics, y is the vector of algebraic variables that typically include the algebraic equations associated with the machine models and the power flow equations, and u is the vector of control variables. The function f is a nonlinear vector function that represents the system differential equations, and g is a vector function that represents the system algebraic equations.

There are two main types of analysis techniques that can be used to evaluate a power system's stability: small-signal stability analysis and transient stability analysis. The method of analysis chosen primarily depends on the type of disturbance being imposed on the system. Here, we focus on the system's response to a small disturbance, so we use small-signal stability analysis.

2.3.1 Small-Signal Stability Analysis

Small-signal stability analysis deals with the ability of a power system to maintain synchronism under small disturbances. An example of a small disturbance is an increase in active and reactive power loads. The disturbances are considered to be sufficiently small such that the non-linear system differential equations can be linearized about an operating point. Modal or eigenvalue analysis can then be performed to evaluate system stability based on the location of the system poles.

Linearization is done by approximating (24) using the first term of the Taylor series expansion at an operating or equilibrium point (x_0,y_0). This leads to the following expression

$$\begin{bmatrix} \Delta\dot{x} \\ 0 \end{bmatrix} = \begin{bmatrix} D_x f & D_y f \\ D_x g & D_y g \end{bmatrix} \begin{bmatrix} \Delta x \\ \Delta y \end{bmatrix} \tag{25}$$

where each of the D terms represent the Jacobian matrices of the vector functions with respect to the *x* and *y* variables at the operating point. The deltas represent small increments with respect to the operating point as shown below.

$$\Delta x = x - x_o ; \Delta y = y - y_o \tag{26}$$

We can combine the differential and algebraic equations presented in Section II into the state-space representation

$$\Delta\dot{x} = A_{sys}\Delta x + B\Delta u \tag{27}$$

where x is the vector of state variables, u is the vector system inputs, A_{sys} is the system state matrix, and B is the input matrix. Based on the system models discussed in the previous section,

$$x = [x_{synch,i}\ x_{AVR,i}\ x_{TG,j}\ x_{DFIG,k}]^T$$

$$u = [u_{AVR,i}\ u_{TG,j}]^T$$

$$\text{where } i = [1, 2, \ldots, n_{synch}] \text{ and } j = [1, 2, \ldots, n_{TG}]$$

It is assumed that every synchronous generator has an AVR attached to it, but does not necessarily have a TG attached to it. A_{sys} is computed using the following equation, and it is assumed that $D_y g$ is non-singular. If $D_y g$ is singular, then a singularity induced bifurcation point occurs. More details on this exception can found in [4].

$$A_{sys} = D_x f - D_y f (D_y g)^{-1} D_x g \tag{28}$$

The eigenvalues of the A_{sys} matrix are then analyzed for stability. The system is considered locally stable about the equilibrium point if all of the system's eigenvalues are in the left-half plane, i.e. all of the eigenvalues have a negative real part. The system is considered unstable if there are any eigenvalues in the right-half plane. It is important to note that there is an exception where zero eigenvalues exist while the power system is still considered stable. This can occur for two reasons: either there is no infinite bus, and the

rotor angles are instead referred to a common reference frame, or an assumption is made that generator torques are independent of speed deviation [11].

In addition to eigenvalue analysis, the step response of the linearized system can also be analyzed to get a graphical representation of the system over time in order to see how long it takes for the system to reach a steady state and to see the oscillatory behavior of the system when subject to a step input.

2.4 IEEE 14-Bus System

The IEEE 14-bus system shown in Figure 2.9 below is a common benchmark used to evaluate the impact of various disturbances on power systems. In the system, buses 1 and 2 are synchronous generator buses that provide active power to the 11 loads in the system. 615 MW of power are generated at bus 1, and 60 MW of power are generated at bus 2. Synchronous compensators are located at buses 3, 6, and 8, and they either generate or absorb reactive power based on the balancing needs of the system. Details on all of the IEEE 14-bus system parameters can be found in the appendix of [4].

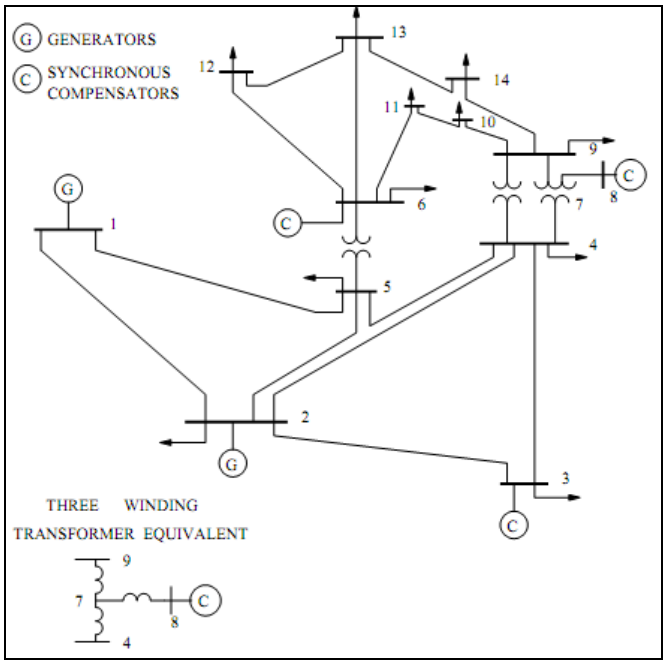

Figure 2.9: IEEE 14-Bus System

Here, we evaluate the impact that a power system with deep penetration of wind has on the small-signal stability of the system before and after various turbine governor controllers are applied. DFIG wind turbines are connected to buses 1 and 2 with 50% power penetration. This equates to 307.5 MW of rated wind power at bus 1 and 30 MW of power at bus 2. The remaining power is generated using synchronous generators.

In order to analyze small-signal stability effects, each load's active and reactive power is increased by 20%. In each case, it is assumed that the AVR gain remains constant in order to focus on the turbine governor effects of the system. The example is analyzed and simulated using the power systems analysis toolbox (PSAT) and controls toolbox within MATLAB [12].

2.4.1 Small-Signal Disturbance Effect

The 20% increase in load active and reactive power creates a drop in bus voltage across the system. The drop in bus voltage can be seen from the results obtained by doing a power flow analysis in Table 2.1 below.

No Disturbance	**Load Power Disturbance Applied**
Bus Voltage (p.u)	***Bus Voltage (p.u)***
1.06	*1.06*
1.045	*1.045*
1.01	*1.01*
1.012	*1.005*
1.016	*1.01*
1.07	*1.07*
1.0493	*1.0429*
1.09	*1.09*
1.0328	*1.0231*
1.0318	*1.0222*
1.0471	*1.042*
1.0534	*1.05*
1.047	*1.042*
1.021	*1.009*

Table 2.1: Bus voltages before and after applied disturbance

Step-response simulations are presented in order to show the various effects of the turbine governor on the frequency of the synchronous generators. Figures 2.10 and 2.11 below show the response comparing the effects before and after the inclusion of turbine governors into a system with no load disturbance. We can see that the inclusion of turbine governors has a strong effect on the damping of oscillations. The same is true in Figures 2.12 and 2.13 where the 20% load disturbance is applied to the system. If we compare those figures to the Figures 2.10 and 2.11, we can see that the disturbance has the effect of increasing the amplitude of the oscillations.

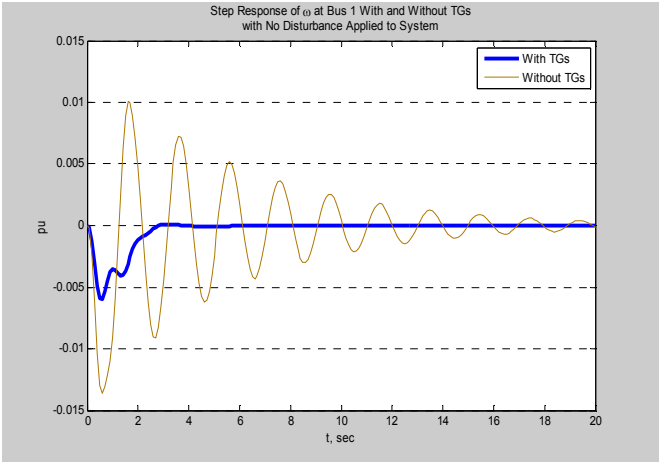

Figure 2.10: Bus 1 Step Response Comparison – With and Without TGs with No Disturbance Applied to System

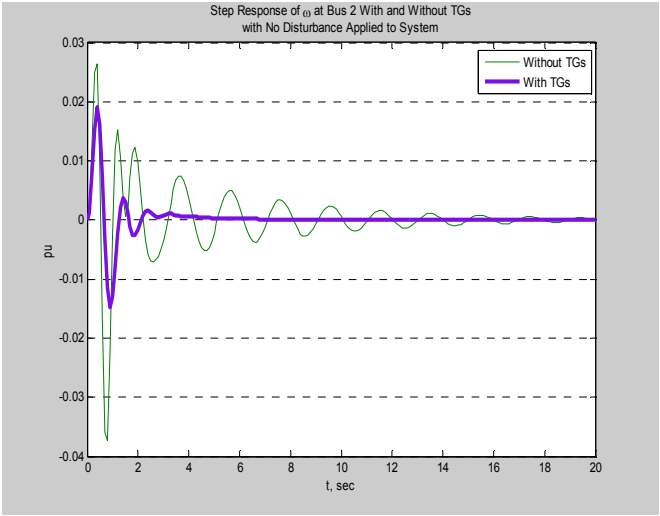

Figure 2.11: Bus 2 Step Response Comparison – With and Without TGs with No Disturbance Applied to System

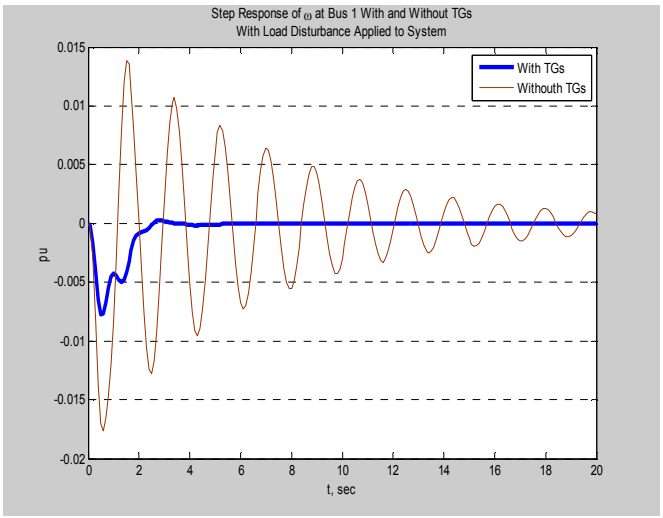

Figure 2.12: Bus 1 Step Response Comparison – With and Without TGs with Load Disturbance Applied to System

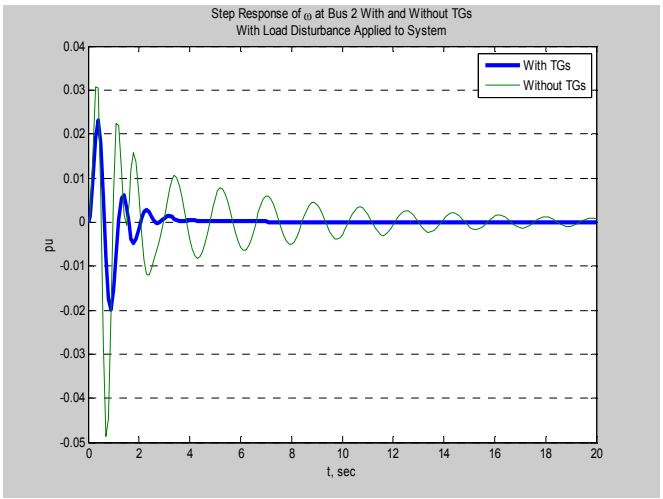

Figure 2.13: Bus 2 Step Response Comparison – With and Without TGs with Load Disturbance Applied to System

We can also compare the eigenvalues of the system to determine the effects of the turbine governors on the movement of the poles with respect to the imaginary axis. The table below compares the eigenvalues of the load disturbance case described above without turbine governors are applied and after they are applied with an R value of 0.05.

State Variable	**Without TGs**				**With TGs**		
	Real	**Imag**	**Freq (Hz)**		**Real**	**Imag**	**Freq (Hz)**
ω_{synch1}	*-0.15*	*3.44*	*0.55*		*-0.83*	*2.50*	*0.42*
ω_{synch1}	*-0.15*	*-3.44*	*0.55*		*-0.83*	*-2.50*	*0.42*
ω_{synch2}	*-2.45*	*9.28*	*1.53*		*-4.13*	*7.06*	*1.30*
ω_{synch2}	*-2.45*	*-9.28*	*1.53*		*-4.13*	*-7.06*	*1.30*

Table 2.2: Eigenvalue Analysis Comparison – Power System with Load Disturbance With TGs vs Without TGs

Next, we look to study the effects of using different droop gain on the system. Figure 2.14 below shows the variation in effect when R = 0.02 is used compared to R = 0.05. It is evident that a lower droop will have a more positive effect on the damping of the system.

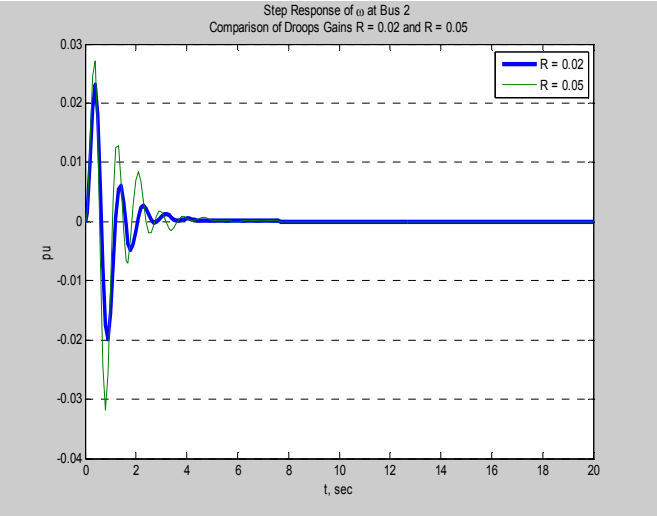

Figure 2.14: Bus 2 Step Response Comparison – Droop of 0.02 vs 0.05

We can also see the difference in the effect of the droop when comparing the eigenvalues of the two cases.

State Variable	**R = 0.05**				**R = 0.02**		
	Real	**Imag**	**Freq (Hz)**		**Real**	**Imag**	**Freq (Hz)**
ω_{synch1}	*-0.83*	*2.50*	*0.42*		*-30.44*		
ω_{synch1}	*-0.83*	*-2.50*	*0.42*				
ω_{synch2}	*-4.13*	*7.06*	*1.30*		*-22.27*	*5.71*	*3.66*
ω_{synch2}	*-4.13*	*-7.06*	*1.30*		*-22.27*	*-5.71*	*3.66*

Table 2.3: Eigenvalue Analysis Comparison of Power Systems with Different Droops

Here, we see a substantial difference in the effect of reducing the droop by 3 %. This can be expected since frequency and droop are directly proportional based on Equation (6). A tighter regulation would equate to less frequency deviation allowed in the system for the same load disturbance.

Finally, we look at the effect of tuning the droop based on the methodology discussed in Section II Part D and the IEEE 14-bus system described in this section. We assume that the system is operating under a frequency deviation, $\Delta\omega$, of 0.025 pu, and that this frequency deviation will hold true for all cases. We define Case 1 to be when all of the power is being generated by the synchronous generators, and Case 2 to be when we include the induction generators at 50% power into the system. For case 1, we assume that the turbine governors are initially tuned to a droop value of 0.05 for a steady-state power output in order to make Equation (7) valid. In the event of a 20% load disturbance on the original system, the droop value would need to be tuned to 0.0417 to satisfy (7). We can use Equations (21-23) to solve case 2 when the wind power is introduced. Based on the equations, $\Delta P_Y = 0.1$, $\Delta P_N = 0.1$, and R would need to be tuned to 0.0455 to provide a frequency deviation of 0.025 pu. Figure 2.15 below shows the step response comparison of the synchronous generator frequency at Bus 2 two cases. We can see that the tuned TGs with the integration of wind dampen the system more favorably than in the first case where tuned TGs are applied to a system with only synchronous generators.

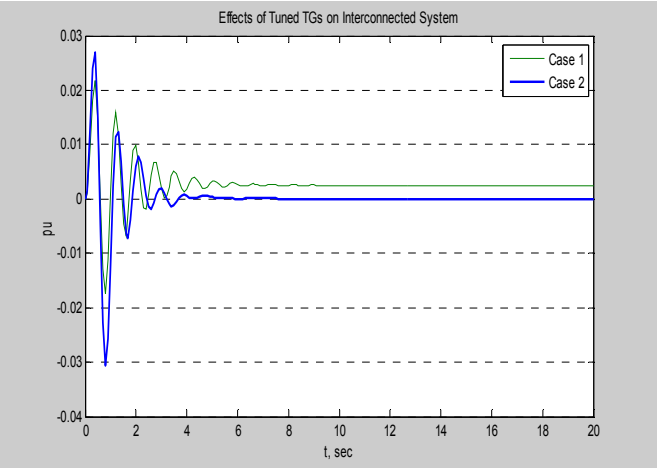

Figure 2.15: Bus 2 Step Response Comparison – Case 1 vs Case 2

Chapter 3

Transient Stability Effects of Modified Transmission Line Configurations on Power Systems with Integration of Wind Power

Previous transient stability studies investigating the effects of wind power integration into a conventional power system assume the insertion point of the wind-generating units to be at the same bus and interconnection voltage as the synchronous generators they are substituting or complementing. While this assumption offers preliminary results into the effects of the wind on the existing system, important points about the physical distance and interconnection voltage of the wind farms with respect to the conventional power system are neglected. This chapter analyzes the effects of integrating doubly-fed induction wind turbine generators through different transmission line configurations and at different buses. The IEEE 14-bus test system is used in order to compare results with previous work. Results show that connecting the wind through transmission lines and to different buses introduces a delay in the oscillatory response of the synchronous generator speed, and bus voltage oscillations are also affected. Results also show that there is no significant effect on the base cases when using different interconnection voltages to connect the wind. The results of this study can be used by power system operators when deciding how to connect wind farms to an existing power network when optimizing for stability response to a large fault. Overall, wind farms should be connected through additional transmission lines to buses near where synchronous generators are located and further away from loads and higher risk fault areas.

3.1 Introduction

As power generated from wind has continued to grow over the last couple of decades, many studies have investigated the modeling of the different wind turbine generators and their effects on power system stability. Typically, these studies have focused heavily on the assumptions taken in the modeling of the wind turbine generator and it's associated controls [9],[5]. There has been substantially less focus placed on the assumptions taken in the modeling of the power system. Almost all studies use a single-machine infinite bus, a small 3-bus system, or the traditional IEEE 14 or 39-bus systems to validate a wind turbine generator model or perform analysis on the integration of wind into the grid [13-14]. While using these power systems can offer insights, they also have particular assumptions that can greatly impact the outcome of the analysis. This chapter attempts to bring one of these assumptions to light in an effort to encourage researchers to develop better power system models that truly represent how large wind farms are integrated into the grid. The common assumption that is challenged in this chapter is the insertion of doubly-fed induction generators (DFIGs) at the original synchronous generator bus location when simulating the transient stability effects of wind power.

Large wind farms that are connected directly to the transmission system are typically located offshore or in remote areas due to their size and lack of aesthetic appeal. Also, the large wind farms are often not linked to the rest of the power system through the same interconnection voltage as the synchronous generators. In both of these cases, additional transmission lines and transformers are needed in order to properly integrate the wind farms into the power system. This chapter analyzes the transient stability effects of these power systems when these assumptions are taken into account. Based on the results, conclusions are made regarding the optimal way to connect doubly-fed induction wind turbine generators (DFIGs) to an existing power system for the purposes of providing enhanced transient stability in the presence of large disturbances.

Well-known transmission line, transformer, and generator models are summarized in Section II. The integration of these models into a complete power system model is provided in Section III. This section also provides an overview of transient stability analysis. In Section IV, the IEEE 14-bus test system and the various transmission line modifications of interest are presented. Simulation results comparing the transient stability effects of the modifications are also shown in Section IV. Concluding remarks are provided in Section V.

3.2 Line, Transformer, and Generator Modeling

This section summarizes the well-known models used to represent transmission lines and transformers for power system studies. Synchronous generators and DFIG generators used to represent wind turbines are also summarized. All of the individual components are combined into a complete power system model using a set of differential-algebraic equations, and this integration is discussed.

3.2.1 Transmission Line and Transformer Models

As mentioned in [4], a transmission line is defined as short if it is less than 1500 km. Short transmission lines can be represented as a π lumped model as shown in Figure 3.1 below.

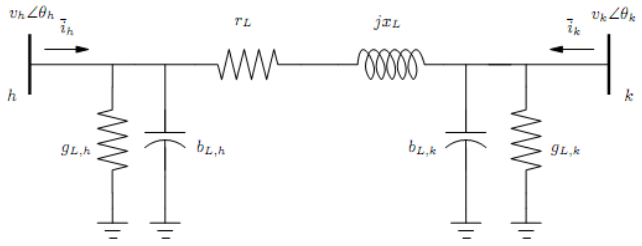

Figure 3.1: Transmission Line π Model

In the figure above, r_L and x_L represent the lumped series resistance and reactance respectively. g_L and b_L represent conductances and susceptances with the subscripts h and k denoting the sending-end and receiving-end respectively. All derivations and assumptions for calculating these variables can be found in [4].

The complex powers injected at each node are represented by the following equations.

$$\bar{s}_h = \bar{v}_h \bar{i}_h^* \tag{29}$$

$$\bar{s}_k = \bar{v}_k \bar{i}_k^* \tag{30}$$

where the injected currents $\bar{i}_h$ and $\bar{i}_k$ are represented using the following equations.

$$\begin{bmatrix} \bar{i}_h \\ \bar{i}_k \end{bmatrix} = \begin{bmatrix} \bar{y}_L + \bar{y}_{L,h} & -\bar{y}_L \\ -\bar{y}_L & \bar{y}_L + \bar{y}_{L,k} \end{bmatrix} \begin{bmatrix} \bar{v}_h \\ \bar{v}_k \end{bmatrix} \tag{31}$$

The admittances, represented by the $\bar{y}$ variable in the above matrix, is related to the conductances and susceptances found in Figure 1 using the following equation.

$$\bar{y}_L = g_L + jb_L \tag{32}$$

The admittances for each transmission line are used for building the network admittance matrix $\bar{Y}$. The network admittance matrix is then used in the power flow equations, and this has an effect on the state matrix that is analyzed for stability. This is discussed in more detail in Section III.

A transformer can best be described as a device that transfers electrical energy through inductively coupled conductors with the ability to step-up or step-down the voltage using the number of turns on the inductor coil windings. Transformers can be modeled as a transmission line with a series impedance and a shunt admittance at the sending-end bus that models iron losses and magnetizing susceptance. The main difference in modeling the transformer and transmission line is that transformers have a complex nominal tap ratio $me^{j\phi}$ that allows modifying the magnitude and phase angle of the bus voltage sending and receiving ends [4].

3.2.2 Synchronous Generator and DFIG Models

Synchronous machine models are used to represent conventional thermal plants. The most basic model is the classical model, which can be represented as a second order system with the following differential equations

$$\dot{\delta} = \Omega_b(\omega - 1) \tag{29}$$

$$\dot{\omega} = \frac{(p_m - p_e - D(\omega - 1))}{M} \tag{30}$$

where

δ : rotor angle

ω : rotor speed

Ω_b : base frequency

p_m, p_e : mechanical power, electrical power

D : damping coefficient

M : mechanical starting time ($M = 2H$)

H : inertia constant

The drawback of the classical 2nd order model is that it neglects all electromagnetic dynamics. Higher order models that include transient and subtransient phenomena are needed for stability analysis. In this chapter, we use a 6th-order model to represent the synchronous machines. The 6th order model is described by Equations (33) and (34) along with differential equations for transient voltages $\dot{e}'_q$ and $\dot{e}'_d$ and subtransient voltages $\dot{e}''_q$ and $\dot{e}''_d$. These variables represent the dynamics of the dc field winding and of the rotor core induced currents and the fast dynamics of damper windings respectively. Full derivation and details on this model can be found in [6-7]. Model comparisons, detailed modeling, and the explanation of assumptions for higher-order versus reduced-order models can be found in various references [4-6].

In addition to the six differential equations, the machine model also has six algebraic equations for the following variables: active power p, reactive power q, bus voltage magnitude v, bus voltage angle θ, mechanical power p_{m} and field voltage v_{f}. Complete details on the algebraic equations can be found in [4],[6].

The general structure of a DFIG wind turbine model and it's associated controls was shown in Figure 2.8. It is shown again below in Figure 3.2 for convenience.

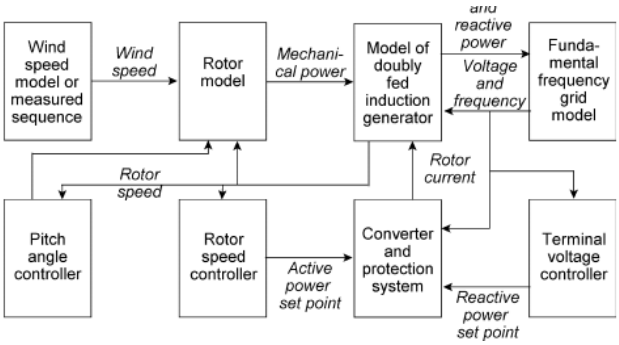

Figure 3.2: General DFIG Wind Turbine Model with Associated Controls

The equation of motion for the rotor modeled as a single shaft is described by the first-order differential equation shown below.

$$\dot{\omega}_m = \frac{\tau_m - \tau_e}{2H_m} \tag{31}$$

where ω_m is the rotational speed, τ_m and τ_e are the mechanical and electrical torques respectively, and H_m is the mechanical inertia constant.

The wind speed is an input to the rotor model. The rotor model assumes an algebraic relationship between the wind speed, v_w and the mechanical power extracted from the wind, p_w as described below where c_p is a performance coefficient function and A_r is the area swept by the rotor [9].

$$p_w = \frac{\rho}{2} c_p(\lambda, \theta) A_r v_w^3 \tag{32}$$

Mechanical power is then related to mechanical torque using the following equation.

$$\tau_m = \frac{p_w}{\omega_m} \tag{33}$$

Since converter dynamics are fast with respect to electromechanical transients, their models can be highly simplified. The converter is modeled as an ideal current source where the d and q-axis rotor currents, i_qr and i_dr, are state variables used for voltage and rotor speed control respectively. A pitch angle controller uses the actual value of the rotor speed to control the blade pitch angle. The reader is referred to [9] for more detailed equations on the controls associated with the DFIG wind turbine and the wind speed model.

3.3 System Model and Transient Stability Analysis

This section discusses the integration of the individual device models discussed in Section II into a power system model. The methodology for performing transient stability analysis is also discussed.

3.3.1 Integrated Power System Model

The non-linear differential and algebraic equations that represent the individual device models can be combined to create a system model. The general equations are shown below [10]

$$\begin{bmatrix} \dot{x} \\ 0 \end{bmatrix} = \begin{bmatrix} f(x,y) \\ g(x,y) \end{bmatrix} \tag{34}$$

where x is the vector of state variables that typically include the machine model dynamics and controller dynamics and y is the vector of algebraic variables that typically include the algebraic equations associated with the machine models, transmission line models, and the power flow equations. The function f is a nonlinear vector function that represents the system differential equations, and g is a vector function that represents the system algebraic equations.

The complete Jacobian matrix of Equation (38) can be written as follows

$$\begin{bmatrix} \partial\dot{x} \\ 0 \end{bmatrix} = \begin{bmatrix} f_x & f_y \\ g_x & g_y \end{bmatrix} \begin{bmatrix} \partial x \\ \partial y \end{bmatrix} \tag{35}$$

where f_x and f_y are the Jacobian terms associated with the partial derivatives of the state-space equations with respect to the state and algebraic variables, while g_x and g_y represent the Jacobian terms associated with the partial derivatives of the algebraic equations with respect to the state and algebraic variables. We can then solve for the state matrix, A_s, as follows

$$A_s = f_x - f_y g_y^{-1} g_x \tag{36}$$

where it is implicitly assumed that there are no singularity-induced bifurcations in the system, so g_y is not singular. Based on the three previous equations, we can see that the proposed method of modifying the transmission lines will have an effect on the state matrix

of the system in different ways. The modified power system with additional transmission lines or the insertion of wind farms at different locations will yield different power flow equations that will change the algebraic equations that make up g. Additionally, the system of variables making up x will be different due to the modified number of transmission lines and transformers in the system. In summary, the proposed changes will modify f_y and g_x , and g_y.

3.3.2 Transient Stability Analysis

Transient stability deals with the ability of a power system to maintain synchronism when subjected to a large or severe disturbance [11],[2]. Examples of a large disturbance include loss of generation, loss of a large load, or a transmission line fault. Transient stability analysis looks at the system response to these large disturbances through time domain simulations of a system's state and algebraic variables. Synchronous generator rotor angle and speed as well as bus voltages are some of the system variables typically affected by transient disturbances.

In the event of a large disturbance, the non-linear differential algebraic equations representing the power system can not be linearized about an operating point since the perturbation can not be assumed to be sufficiently small. Instead, numerical integration methods for solving the high-order differential equations are needed. Many different techniques are available, and the most commonly used techniques build off of the explicit forward Euler's method. This method states that

$$x_{i+1} = x_i + \Delta t\, f(x_i, t) \tag{37}$$

at a point in time, t_{i+1} where Δt is the step length that can be fixed or varied from step to step. More details on the various numerical integration methods used in power systems can be found in [4].

The main objective of transient stability analysis is to determine whether or not the system is stable based on the system's time domain simulation response when the numerical integration is solved. If the time domain simulation diverges, then the system is unstable.

Otherwise, the system is stable. The dynamic models associated with the machines that make up the f_x Jacobian are almost always stable on their own. For this reason, the product $f_y g_y^{-1} g_x$ is typically called the degradation matrix, D, since it degrades the stability of the f_x matrix [4]. Since these matrices are the same matrices that are modified when changing the power system configuration, it is important to see how the system's transient stability will change under the new conditions.

3.4 Case Study: IEEE 14-Bus System

In this section, an overview of the IEEE 14-bus test system is provided. Then, different case studies are shown where modifications are made to the test system in order to analyze the effects that various transmission line configurations have on the transient stability of the system when wind power is connected.

3.4.1 IEEE 14-Bus System

The IEEE 14-bus system shown in Figure 2.9 is shown again here in Figure 3.3 for convenience. As discussed previously, this test system is a common benchmark used to evaluate the impact of various disturbances on power systems. In the system, buses 1 and 2 are synchronous generator buses that provide active power to the 11 loads in the system. 615 MW of power are generated at bus 1, and 60 MW of power are generated at bus 2. Synchronous compensators are located at buses 3, 6, and 8, and they either generate or absorb reactive power based on the balancing needs of the system. Details on all of the IEEE 14-bus system parameters can be found in the appendix of [4].

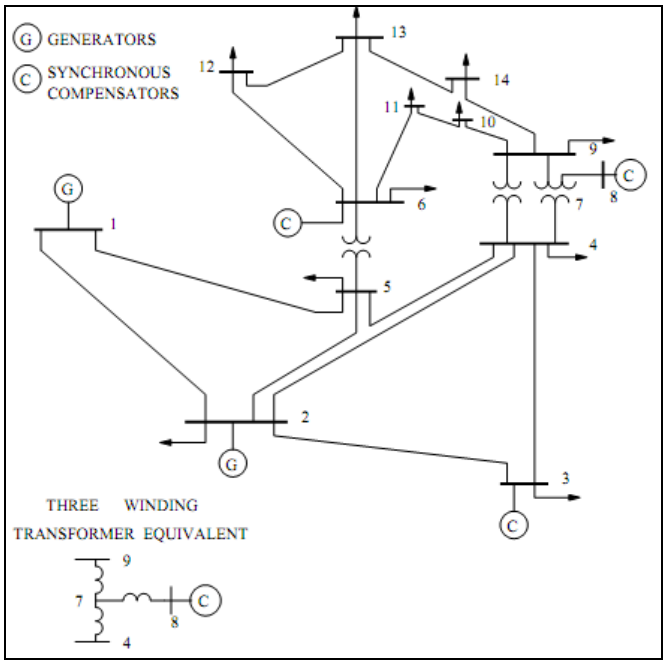

Figure 3.3: IEEE 14-Bus System

3.4.2 Case Studies

There are four different comparisons shown in this section. A diagram of the modifications for each of the comparisons is provided. Each comparison is followed up by analysis in the form of time domain simulations for the synchronous generator speed and voltage at bus 1. The focus is on bus 1 because this is where the majority of generated power occurs in the original test system, and this is where the largest rated synchronous generator is located. These factors make this bus most vulnerable to instabilities due to a transient fault. Additionally, simulations show that the synchronous machines at Buses 1 and 2 oscillate in the same manner, so it would be somewhat redundant to show all of the simulations for the synchronous generator at Bus 2.

In all cases, a three-phase transmission line fault is used as the disturbance. This is simulated through a line 2-4 outage occurring at t = 1 s that is cleared at t = 1.2 s. In all cases, we also assume there is deep penetration of wind. 308 MW of generated wind power is used, which is approximately 50% of the total power generated by the synchronous generator at Bus 1. For each of the cases that include the integration of wind, the synchronous generator power at Bus 1 is reduced to 307 MW. Generally, the main assumption challenged by the following cases is that large wind farms are connected to

synchronous generator buses without the need for additional transmission lines or transformers to account for the distance or interconnection voltages between the different generators. Each case focuses on a specific issue in an attempt to reach a conclusion on the best way to connect wind farms to an existing power system when optimizing for transient stability.

3.4.2.1 Case A – Effects of Adding Wind with and Without TL to Bus 1

In this case, we are interested in analyzing the effects of adding wind to the system at Bus 1 with and without additional transmission lines. Figure 4 below shows the scenarios. For all diagrams, "G" denotes a synchronous generator, "W" denotes a wind farm composed of DFIGs, and "T" denotes a transmission line system. The transmission line system is composed of only transmission lines when the same interconnection voltage between the two buses is used. When the interconnection voltages between the two buses are different, the transmission line system also includes a transformer that either steps up or steps down the voltage. In this case, a 69 kV interconnection is used to connect the wind. Since 69 kV is also the original voltage at Bus 1, no transformer is needed.

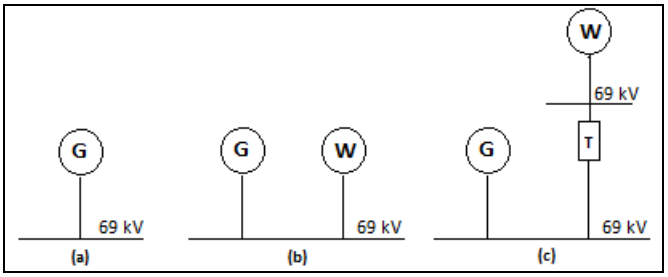

Figure 3.4: Case A – Effects of Adding Wind with and without TL to Bus 1

Figures 3.5 and 3.6 below provide time domain simulations for the different scenarios in Figure 3.4. In all simulations below, the *x*-axis denotes time in units of seconds while the *y*-axis is denoted in per-unit (p.u.) voltage or speed. In Figure 3.5, we can see that the addition of wind power into the system creates more synchronous generator oscillations, but that the oscillations settle more closely around 1 p.u. There is also an apparent shift or delay caused when adding the transmission line.

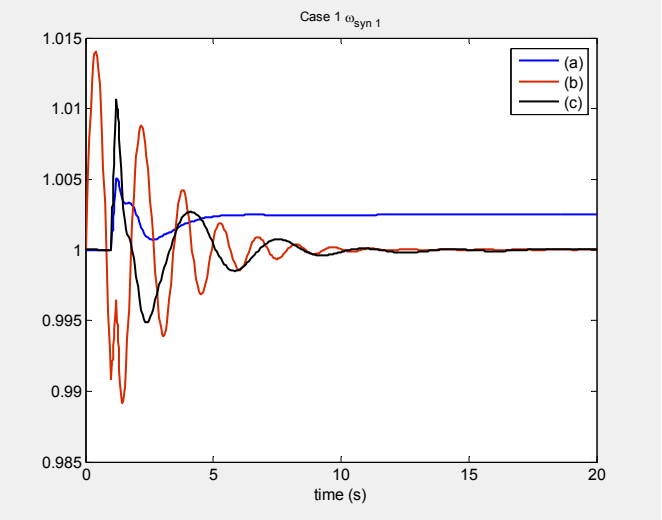

Figure 3.5: Comparing transient stability effects on ω_{syn1} for cases in Fig. 3.4

Figure 3.6 below shows the voltages at Bus 1. The outage at t = 1s causes a large drop in voltage that is recovered shortly thereafter. The added transmission line before connecting the wind power has the effect of reducing the overshoot and damping the oscillation when compared to the case when the wind is connected directly to the synchronous generator bus.

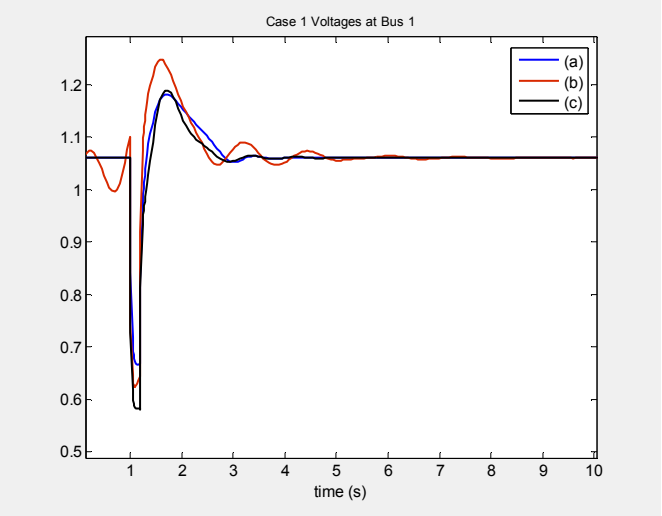

Figure 3.6: Comparing transient stability effects on V_{bus1} for cases in Fig. 3.4

3.4.2.2 Case B – Effects of Adding Wind through Different Interconnection Voltages

In this case, we are interested in analyzing the effects of adding wind to the system at Bus 1 through different interconnection voltages. It is important to investigate this because wind farms may be connected to an existing power system at a different voltage than what the synchronous generators are set at. Figure 3.7 shows the different comparisons. Fig. 3.7(a) is the base case that doesn't require the need for a transformer since the wind is connected at the same interconnection voltage. In the other two cases, a step-down and step-up voltage transformer is needed in addition to the transmission line.

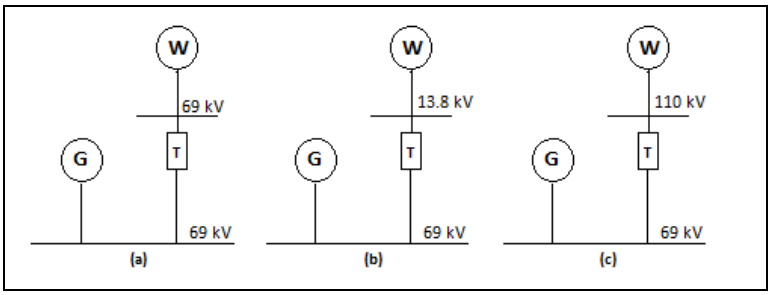

Figure 3.7: Case B – Effects of Adding Wind
through Different Interconnection Voltages

In Figures 3.8 and 3.9 below, we can see that there is not much difference between the three cases. The case with the lowest interconnection voltage creates slightly larger oscillations than the other two cases for both the synchronous generator speed and bus voltage.

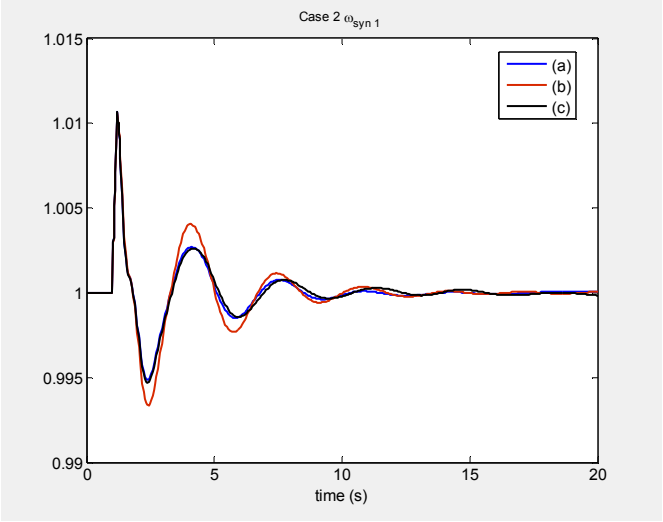

Figure 3.8: Comparing transient stability effects on ω_{syn1} for cases in Fig. 3.7

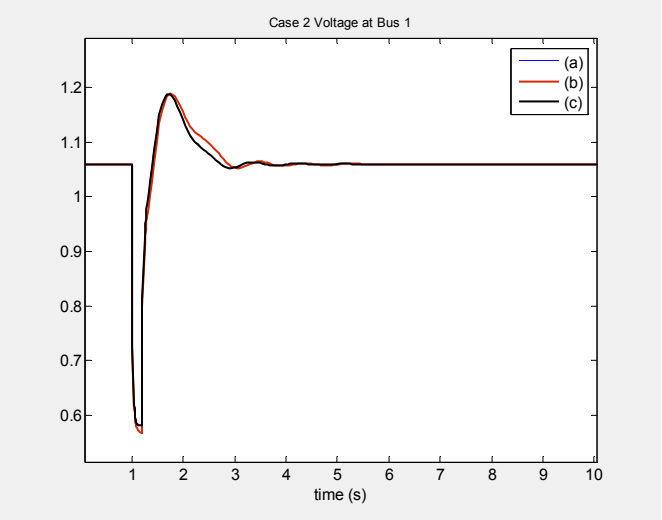

Figure 3.9: Comparing transient stability effects on V_{bus1} for cases in Fig. 3.7

3.4.2.3 Case C – Effects of Adding Wind to Different Buses

Here, we are interested in connecting the wind to different power system buses. It is possible for wind farms to be located near other power system buses and away from the main point of conventional power generation. Figure 3.10 shows the variations. The base case is shown in Fig. 10(a) where the wind is connected to Bus 1. Figs. 3.10(b) and (c) show the wind being connected to Bus 8 and 14 respectively.

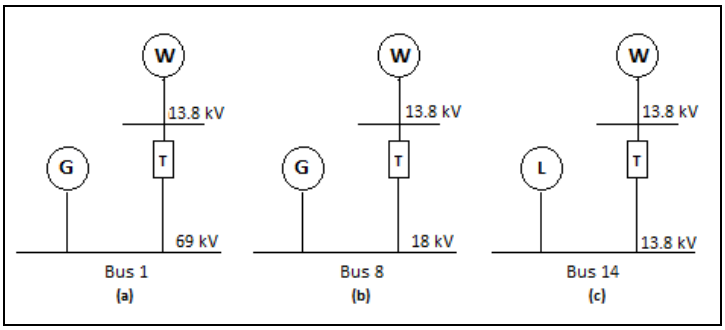

Figure 3.10: Case C – Effects of Adding Wind to Different Buses

Figures 3.11 and 3.12 below show the transient stability effects for Case C. There are significant variations present when analyzing the effects on the synchronous generator speed. Since Case B proved that connecting the wind through different interconnection voltages didn't have a profound effect, we can attribute the variations here to the bus

location. Connecting the wind through Bus 8 shows a phase shift with similarly damped oscillations when compared with the base case. Connecting the wind through Bus 14 shows a more pronounced phase shift with more oscillations. There is not much effect on the bus voltage as seen in Figure 3.12.

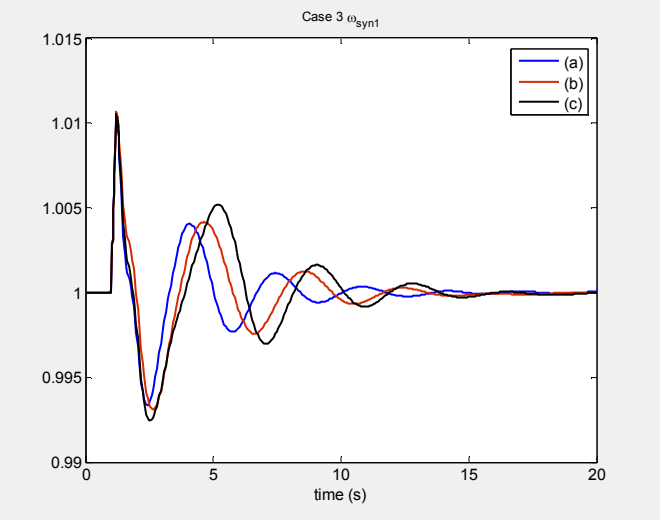

Figure 3.11: Comparing transient stability effects on ω_{syn1} for cases in Fig. 3.10

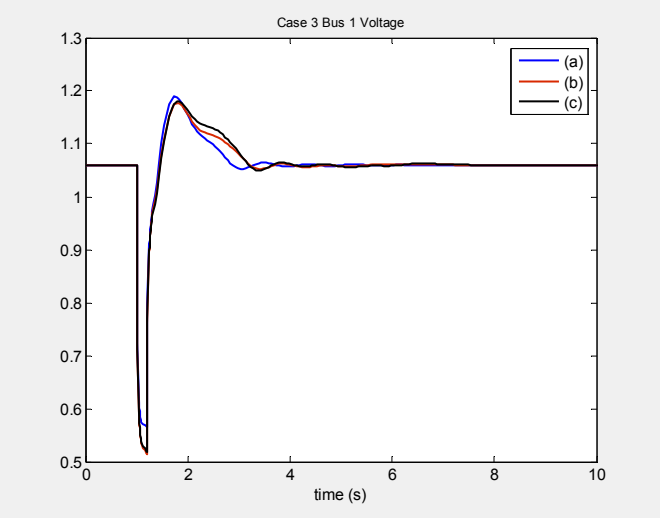

Figure 3.12: Comparing transient stability effects on V_{bus1} for cases in Fig. 3.10

3.4.2.4 Case D – Effects of Adding Wind through Multiple TLs

In this case, we are interested in seeing the effects when the wind generation is fed into two separate buses rather than being channeled into one bus as was shown in the previous cases. This is presented in Figure 3.13 below.

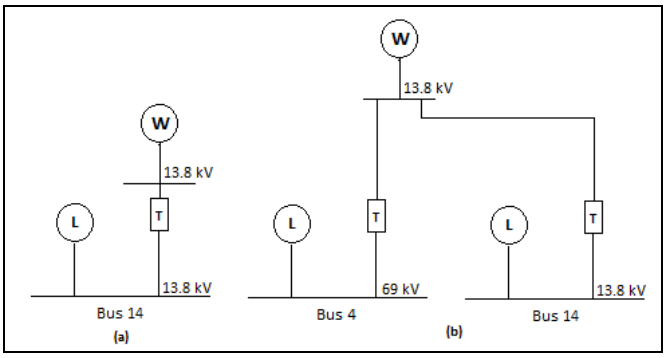

Figure 3.13: Case D – Effects of Adding Wind Through Multiple TLs

The results of running transient stability simulations for Case D are shown in Figures 3.14 and 3.15 below. The topology of connecting the wind through different transmission lines to multiple buses does not seem to have a significant effect on the transient stability of the system.

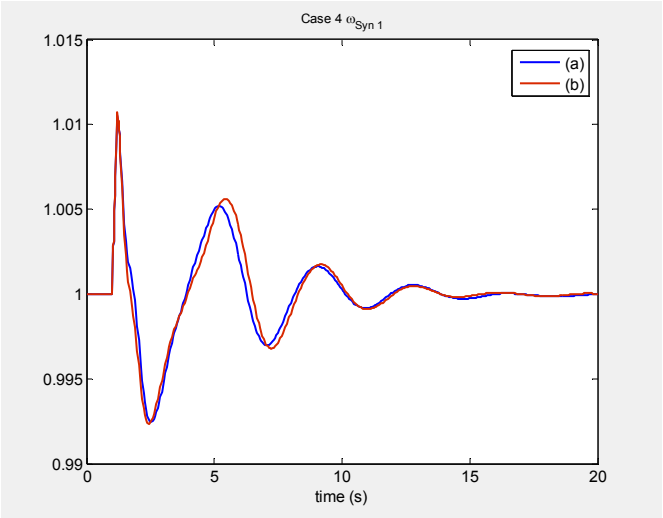

Figure 3.14: Comparing transient stability effects on ω_{syn1} for cases in Fig. 3.13

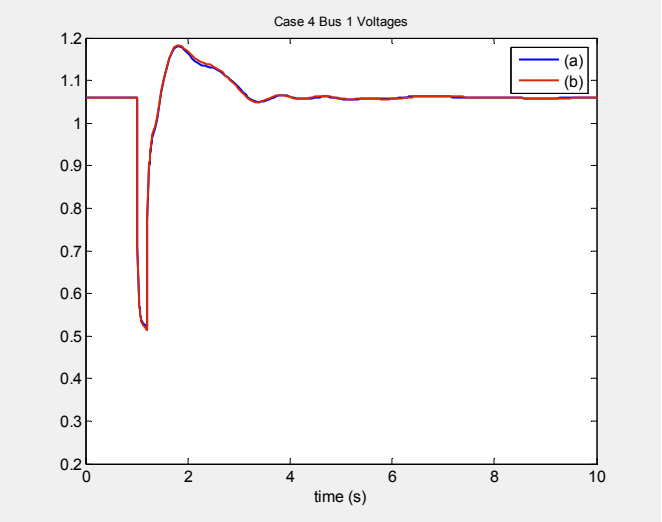

Figure 3.15: Comparing transient stability effects on V_{bus1} for cases in Fig. 3.13

3.4.2.5 Further Discussion

It should also be noted that in all cases, the bus voltages are more negatively affected based on their proximity to where the system fault occurs. This can be seen in Figure 3.16 below where different bus voltages for Case 1(c) are plotted. Bus 4 has the lowest drop in voltage as this is where the fault occurs, and buses connected to Bus 4 have larger voltage drops than buses further away from that bus.

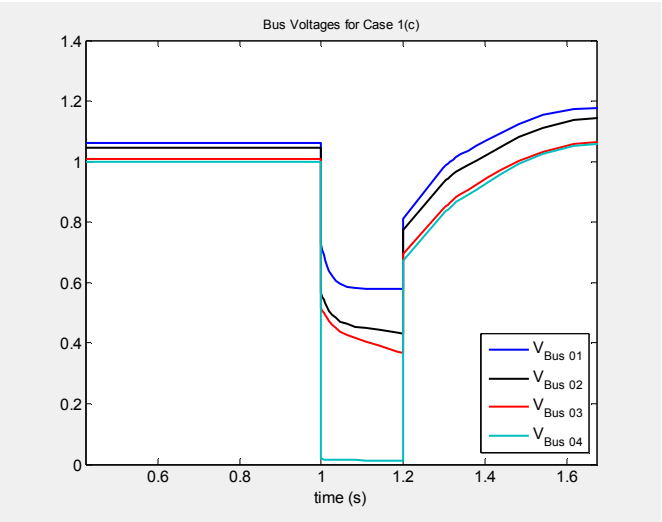

Figure 3.16: Comparing transient stability effects on different bus voltages for cases in Fig. 3.13

Chapter 4

Conclusion and Future Work

4.1 Conclusion

This thesis has studied the small-signal stability effects of the synchronous generator turbine governors in the presence of wind power generation. Under certain assumptions, the wind power generation can actually prove to be beneficial to the overall small-signal stability of the interconnected power system, and the stability can be further enhanced by tuning the turbine governors to account for the substitution or addition of rated wind power in the system.

This thesis has also studied the transient stability effects on a conventional power system when large integration of wind power is connected through various transmission line configuration schemes. Based on the simulation results, connecting the wind power generating units through additional transmission lines both at Bus 1 and at other buses had a noticeable effect on the transient stability of the system (shown in Cases A and C in Section 3.4.2), while varying the interconnection voltage of the wind power to the rest of the system had a negligible effect (shown in Cases B and D). This type of analysis can be used by power system operators when deciding how to best integrate a large wind farm into an already existing power network.

4.2 Future Work

Future work can build upon this thesis in a number of ways. In the case where the effects of turbine governors were analyzed, future work could include studying the impact of a global controllers on the small-signal stability of a power system. The turbine governors are effectively local controllers that can be placed on any number of synchronous generators included in the system. However, a tuned global controller could potentially be programmed optimally to regulate the frequency of all synchronous generators in the presence of large penetration of wind. The feasibility of this issue has yet to be investigated.

In the case where the effects of transmission line configurations were analyzed, future work could include studying the impact of high-voltage DC (HVDC) transmission lines on the transient stability of a power system. Studying the effects of HVDC transmission lines on system stability is important because offshore wind farms and other wind farms located far away from existing power systems utilize high-voltage lines to minimize losses and connect to the grid. There has been some preliminary research done on this, but there is still a great deal of work that needs to be done in building out solid HVDC line models that are easily integrated into current power system software programs. This thesis predominantly used PSAT as a software tool, which includes preliminary HVDC models, but these models have not been tested fully and result in countless singularity and numerical integration issues if the parameters are not configured and set in an exact fashion.

Appendix A

MATLAB Code

The following code is used to simulate the plots in Chapter 2. The only change needed is the name of the .mdl file being used and the number of columns in C based on the number of state variables in the system.

```
%% Plot the step response
clear all

%% initialize PSAT
initpsat
% do not reload data file
clpsat.readfile = 0;

% set data file
runpsat('tgnowind.mdl','data')

% Run the power flow
runpsat('pf')

%% Linearize system
% Compute A and B matrices
fm_abcd;

% Store matrices
A = LA.a;
B = [LA.b_avr LA.b_tg]; %In this case, due to AVRs

% Define the outputs of interest
C = zeros(2,20);
C(1,2) = 1; %synch gen speed 1
C(2,8) = 1;
D=0;

%% Plotting
% Eigenvalues and frequency deviation step response before control
```

```
% Epre = eig(A);
figure(1)
t = 0:0.1:20;
[y, x] = step(A, B, C, D, 1, t);
plot(t,y), grid, xlabel('t, sec'), ylabel('pu')
legend('\omega Bus 1', '\omega Bus 2')
```

Bibliography

[1] T. Ackerman, *Wind Power in Power Systems*. John Wiley & Sons, 2005.

[2] L. L. Grigsby, *The Electric Power Engineering Handbook*. CRC, 2001.

[3] A. J. Wood and B. F. Wollenberg, *Power Generation, Operation, and Control*, vol. 2. Wiley New York, 1996.

[4] F. Milano, *Power System Modelling and Scripting*. Springer Verlag, 2010.

[5] L. Rouco and J. L. Zamora, "Dynamic patterns and model order reduction in small-signal models of doubly fed induction generators for wind power applications," in *Power Engineering Society General Meeting, 2006. IEEE*, 2006.

[6] P. M. Anderson and A. A. Fouad, "Power System Control and Stability," 2003.

[7] J. Machowski, J. Bialek, and J. Bumby, *Power System Dynamics: Stability and Control*. Wiley, 2011.

[8] L. Pereira, J. Undrill, D. Kosterev, D. Davies, and S. Patterson, "A new thermal governor modeling approach in the WECC," *Power Systems, IEEE Transactions on*, vol. 18, no. 2, pp. 819–829, 2003.

[9] J. G. Slootweg, "Wind power: Modelling and Impact on Power System Dynamics," 2003.

[10] R. Z. Minano, A. J. C. Navarro, and F. Milano, "Optimal Power Flow with Stability Constraints."

[11] P. Kundur, N. J. Balu, and M. G. Lauby, *Power System Stability and Control*, vol. 4. McGraw-Hill New York, 1994.

[12] F. Milano, “An open source power system analysis toolbox,” *Power Systems, IEEE Transactions on*, vol. 20, no. 3, pp. 1199–1206, 2005.

[13] J. C. Muñoz and C. A. Cañizares, “Comparative stability analysis of DFIG-based wind farms and conventional synchronous generators,” in *Power Systems Conference and Exposition (PSCE), 2011 IEEE/PES*, 2011, pp. 1–7.

[14] D. Naimi and T. Bouktir, “Impact of wind power on the angular stability of a power system,” *Leonardo Electronic Journal of Practices and Technologies*, vol. 7, no. 12, pp. 83–94, 2008.